European Radiology (2020) 30:6003–6013
https://doi.org/10.1007/s00330-020-07014-1

HEPATOBILIARY-PANCREAS

Gadoxetate-enhanced abbreviated MRI is highly accurate for hepatocellular carcinoma screening

Naik Vietti Violi[1,2,3] · Sara Lewis[1,2] · Joseph Liao[2] · Miriam Hulkower[2] · Gabriela Hernandez-Meza[4] · Katherine Smith[5] · James S. Babb[6] · Xing Chin[2] · Joseph Song[2] · Daniela Said[1,2,7] · Shingo Kihira[2] · Claude B. Sirlin[8] · Scott B. Reeder[9] · Mustafa R. Bashir[10] · Kathryn J. Fowler[8] · Bart S. Ferket[11] · Keith Sigel[12] · Bachir Taouli[1,2]

Received: 10 February 2020 / Revised: 29 April 2020 / Accepted: 5 June 2020 / Published online: 25 June 2020

Abstract

Objectives The primary objective was to compare the performance of 3 different abbreviated MRI (AMRI) sets extracted from a complete gadoxetate-enhanced MRI obtained for hepatocellular carcinoma (HCC) screening. Secondary objective was to perform a preliminary cost-effectiveness analysis, comparing each AMRI set to published ultrasound performance for HCC screening in the USA.

Methods This retrospective study included 237 consecutive patients (M/F, 146/91; mean age, 58 years) with chronic liver disease who underwent a complete gadoxetate-enhanced MRI for HCC screening in 2017 in a single institution. Two radiologists independently reviewed 3 AMRI sets extracted from the complete exam: non-contrast (NC-AMRI: T2-weighted imaging (T2wi)+diffusion-weighted imaging (DWI)), dynamic-AMRI (Dyn-AMRI: T2wi+DWI+dynamic T1wi), and hepatobiliary phase AMRI (HBP-AMRI: T2wi+DWI+T1wi during the HBP). Each patient was classified as HCC-positive/HCC-negative based on the reference standard, which consisted in all available patient data. Diagnostic performance for HCC detection was compared between sets. Estimated set characteristics, including historical ultrasound data, were incorporated into a microsimulation model for cost-effectiveness analysis.

Results The reference standard identified 13/237 patients with HCC (prevalence, 5.5%; mean size, 33.7 ± 30 mm). Pooled sensitivities were 61.5% for NC-AMRI (95% confidence intervals, 34.4–83%), 84.6% for Dyn-AMRI (60.8–95.1%), and 80.8% for HBP-AMRI (53.6–93.9%), without difference between sets (p range, 0.06–0.16). Pooled specificities were 95.5% (92.4–97.4%), 99.8% (98.4–100%), and 94.9% (91.6–96.9%), respectively, with a significant difference between Dyn-AMRI and the other sets ($p < 0.01$). All AMRI methods were effective compared with ultrasound, with life-year gain of 3–12 months against incremental costs of US$ < 12,000.

Electronic supplementary material The online version of this article (https://doi.org/10.1007/s00330-020-07014-1) contains supplementary material, which is available to authorized users.

✉ Bachir Taouli
bachir.taouli@mountsinai.org

[1] BioMedical Engineering and Imaging Institute, Icahn School of Medicine at Mount Sinai, New York, NY, USA

[2] Department of Diagnostic, Molecular and Interventional Radiology, Icahn School of Medicine at Mount Sinai, 1470 Madison Avenue, New York, NY 10029, USA

[3] Department of Radiology, Lausanne University Hospital, Lausanne, Switzerland

[4] Icahn School of Medicine at Mount Sinai, New York, NY, USA

[5] Columbia University, New York, NY, USA

[6] Department of Radiology, New York University Langone Medical Center, New York, NY, USA

[7] Department of Radiology, Universidad de los Andes, Santiago, Chile

[8] Liver Imaging Group, Department of Radiology, UC San Diego Medical Center, 200 West Arbor Drive, San Diego, CA, USA

[9] Department of Radiology, University of Wisconsin, Madison, WI, USA

[10] Department of Radiology, Duke University School of Medicine, Durham, NC, USA

[11] Department of Population Health Science and Policy, Icahn School of Medicine at Mount Sinai, New York, NY, USA

[12] Division of General Medicine, Icahn School of Medicine at Mount Sinai, New York, NY, USA

Conclusions NC-AMRI has limited sensitivity for HCC detection, while HBP-AMRI and Dyn-AMRI showed excellent sensitivity and specificity, the latter being slightly higher for Dyn-AMRI. Cost-effectiveness estimates showed that AMRI is effective compared with ultrasound.

Key Points

- *Comparison of different abbreviated MRI (AMRI) sets reconstructed from a complete gadoxetate MRI demonstrated that non-contrast AMRI has low sensitivity (61.5%) compared with contrast-enhanced AMRI (80.8% for hepatobiliary phase AMRI and 84.6% for dynamic AMRI), with all sets having high specificity.*
- *Non-contrast and hepatobiliary phase AMRI can be performed in less than 14 min (including set-up time), while dynamic AMRI can be performed in less than 17 min.*
- *All AMRI sets were cost-effective for HCC screening in at-risk population in comparison with ultrasound.*

Keywords Carcinoma, Hepatocellular · Mass screening · Magnetic resonance imaging

Abbreviations

AMRI	Abbreviated magnetic resonance imaging
DWI	Diffusion-weighted imaging
Dyn-AMRI	Dynamic AMRI
HBP	Hepatobiliary phase
HCC	Hepatocellular carcinoma
LI-RADS	Liver Imaging Reporting and Data System
NC-AMRI	Non-contrast AMRI
SS EPI	Single-shot echo-planar imaging
SS FSE	Single-shot fast spin echo-planar imaging
Wi	Weighted imaging

Introduction

Hepatocellular carcinoma (HCC) is the fastest growing cause of cancer deaths in the USA [1]. To enable early detection of potentially curable HCC, clinical practice guidelines recommend semi-annual screening with abdominal ultrasound (US) in at-risk populations [2, 3]. However, US has limited sensitivity for detecting small HCC, especially in patients with large body habitus and/or advanced cirrhosis [4, 5]. To improve the performance of imaging screening, many centres perform CT or MRI. While these provide higher sensitivity than US, they are not optimal for HCC screening and surveillance [6, 7] because of higher cost, radiation exposure (for CT), and long exam duration for MRI (between 20 and 40 min). Therefore, current practice guidelines do not advocate the use of CT or MRI for HCC screening and surveillance [2, 3].

Motivated to provide a more sensitive screening method, several investigators have recently reported the use of novel abbreviated MRI (AMRI) protocols. AMRI consists of only a few select MRI sequences for targeted questions such as HCC surveillance and aim for a reduction in time while keeping acceptable diagnostic performance [8]. Several combinations of MRI sequences have been proposed, including a non-contrast (NC)-AMRI combining T2-weighted imaging (T2wi) and diffusion-weighted imaging (DWI) [9–12], gadoxetate-enhanced hepatobiliary phase (HBP)-AMRI with T1wi and T2wi with/without DWI [10, 13–15], or dynamic imaging (Dyn)-AMRI with an extracellular gadolinium-based contrast agent [16, 17]. HBP-AMRI has reported sensitivity of 75.9–95.9% and specificity of 90.2–100% for HCC detection [10, 13]. NC-AMRI using DWI has recently shown a sensitivity of 85.5% and a specificity of 94.6% in a small study [10], while a recent retrospective analysis of prospective acquired data demonstrated superiority of NC-AMRI compared with US (sensitivity 79.1% vs. 27.9% respectively, $p < 0.01$) [12]. All these previous studies assessed reconstructed AMRI protocols from full contrast-enhanced MRIs (using gadoxetate or extracellular contrast), with several reporting high HCC prevalence (up to 85.9%), as most were not performed in the context of screening or surveillance. In addition, the optimal combination of sequences and the need and type of contrast agent for AMRI protocols need to be established.

Our primary objective was to compare the performance of 3 different AMRI sets extracted from a complete gadoxetate-enhanced MRI obtained for HCC screening. Our secondary objective was to perform a preliminary cost-effectiveness analysis, comparing each AMRI set to published US performance for HCC screening in the USA [18].

Material and methods

Patients

This was a single-centre HIPAA- and GDPR-compliant retrospective study from a single institution (Icahn School of Medicine at Mount Sinai). The local Institutional Review Board approved the study and waived signed informed consent. Our electronic imaging database was queried for the year 2017 for consecutive patients who underwent in-house MRI for HCC screening/surveillance. An analysis of our imaging screening data for the year 2017 showed that MRI was used as a first-line modality for HCC screening in > 50% of patients, due to referring physician preferences (unpublished data). Inclusion criteria were adult patients (≥ 18 years) with cirrhosis of any

aetiology and patients with chronic hepatitis B without cirrhosis who underwent a complete gadoxetate-enhanced MRI for HCC screening at our institution. According to the AASLD (American Association for the Study of Liver Diseases) criteria for HCC screening [2], patients with Child-Pugh class C were included if listed for transplantation. When patients underwent multiple MRI examinations in 2017, only the first MRI performed during 2017 was assessed. Among 415 initial patients, 178 were excluded (Fig. 1).

MRI acquisition and extraction of AMRI sets

All MRI examinations were performed with clinical systems, using a standard liver dedicated protocol with injection of a fixed dose of 10 mL of gadoxetate disodium (Eovist/Primovist, Bayer Healthcare). Details on the imaging systems and parameters are provided in the supplementary materials.

Three AMRI sets were extracted from the complete gadoxetate-enhanced liver MRIs and assessed separately: (1) NC-AMRI, including axial non-fat-suppressed T2wi SS FSE (single-shot fast spin echo-planar imaging) + axial fat-suppressed SS EPI (single-shot echo-planar imaging) DWI, (2) Dyn-AMRI, including axial T2 SS FSE + axial DWI + axial dynamic contrast-enhanced fat-suppressed 3D T1wi (VIBE/LAVA; unenhanced, early and late arterial phases, portal venous and transitional phases), and (3) HBP-AMRI, including axial T2wi SS FSE + axial DWI + axial fat-suppressed 3D T1wi (VIBE/LAVA) HBP (at 20 min post contrast injection). T2wi and DWI were included on all sets: T2wi was used to improve lesion characterisation (particularly for cysts and haemangiomas) and DWI has shown value for HCC detection [19, 20].

The estimated acquisition times are listed for each AMRI protocol and each of the main representative systems from our institution in Table 1, and include a conservative estimate of 10 min of set-up time (including patient positioning on the table, sequence set-up, and exam termination) based on our clinical practice. On average, these were below 14 min for NC-AMRI and HBP-AMRI, and below 17 min for Dyn-AMRI, while the average acquisition time for complete gadoxetate MRI was approximately 34 min (Suppl Table 1). Details on acquisition parameters are provided in the supplementary material.

Image analysis

Two independent radiologists (J.L. and S.L., with 3 and 10 years of expertise in abdominal radiology, respectively) reviewed the 3 AMRI sets in two separate sessions separated by at least 6 weeks to reduce recall bias. Patients and sessions were reviewed in random order.

In one session, NC-AMRI was assessed, followed immediately by the HBP-AMRI. NC-AMRI and HBP-AMRI were scored on a per-patient basis using a composite scoring system adapted from the US Liver Imaging Reporting and Data System (LI-RADS) for HCC screening [21]: negative (no observation or definitely benign observations), subthreshold (≥ 1 lesions < 10 mm and not clearly benign), positive (≥ 1 nodules ≥ 10 mm or distinctive area(s) of heterogeneity not attributable to cirrhosis, cysts, or haemangiomas). A patient was considered positive when ≥ 1 lesion was scored HCC-positive and was considered HCC-negative when no lesion was found or lesion(s) found was (were) scored "subthreshold."

In the other session, Dyn-AMRI was assessed on a per-observation basis. Up to 5 observations per patient were selected based on the largest size. For each selected observation (excluding cysts), readers recorded the observation size and location (Couinaud segment and series/image location) and assigned a LI-RADS v2018 category [22]. Scores were then collapsed to a per-patient basis so that patients with LI-RADS 5 lesions were considered HCC-positive; all other patients were

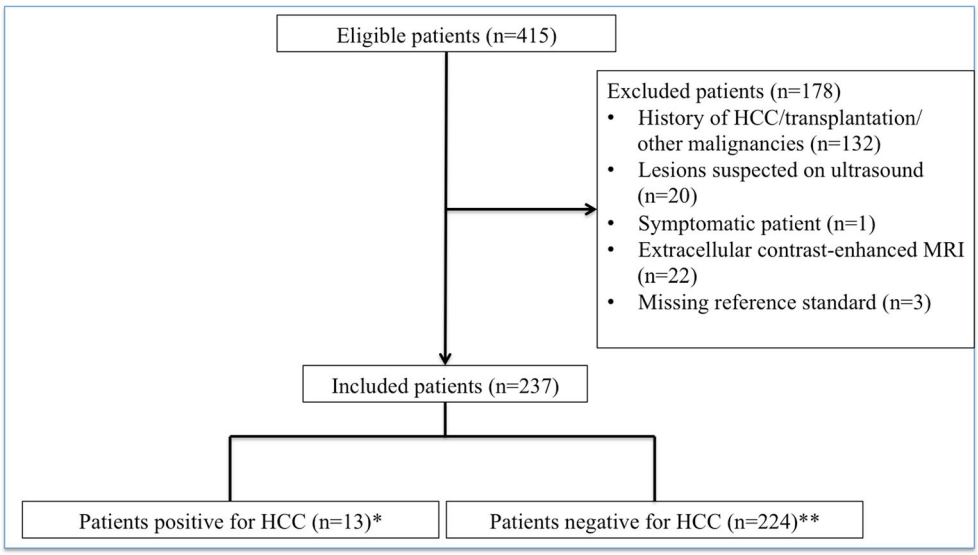

Fig. 1 Flowchart of the study population. Patients positive for HCC include patients with HCC LI-RADS 5 ($n = 11$) and biopsy-proven HCC (categorised as LI-RADS 4 and M, $n = 2$) (indicated by a single asterisk symbol). Patients negative for HCC include patients with cholangiocarcinoma ($n = 1$), benign lesions ($n = 42$), indeterminate lesions ($n = 3$), and no liver lesion ($n = 178$) (indicated by double asterisk symbols)

Table 1 Reconstructed AMRI protocols with corresponding acquisition times (AT) (min:s) (including mean AT and range)

Sequence	Siemens 1.5 T	Siemens 3 T	GE 1.5 T	GE 3 T
NC-AMRI				
Localiser	00:18	00:18	00:22	00:22
Axial T2 HASTE	00:42	00:32	00:30	00:30
Axial DWI	01:28	01:28	03:42	02:00
Set-up time	10:00	10:00	10:00	10:00
Total AT NC-AMRI	12:28	12:18	14:34	12:52
Mean (range) AT NC-AMRI	13:03 (12:18–14:34)			
HBP-AMRI				
Localiser	00:18	00:18	00:22	00:22
Axial T2 HASTE	00:42	00:32	00:30	00:30
Axial DWI	01:28	01:28	03:42	02:00
Axial T1 HBP 20 min	00:11	00:12	00:13	00:12
Set-up time	10:00	10:00	10:00	10:00
Total AT HBP-AMRI	12:39	12:30	14:47	13:04
Mean (range) AT HBP-AMRI	13:15 (12:30–14:47)			
Dyn-AMRI				
Localiser	00:18	00:18	00:22	00:22
Axial multiphase T1 pre-contrast	00:11	00:12	00:13	00:12
Care bolus/timing	01:01	01:01	00:20	00:20
Axial multiphase T1 AP1	00:11	00:12	00:13	00:12
Axial multiphase T1 AP2	00:11	00:12	00:13	00:12
Delay	00:38	00:36	00:34	00:36
Axial multiphase T1 PVP	00:11	00:12	00:13	00:12
Axial T2 HASTE*	00:42	00:32	00:30	00:30
Delay	01:07	01:16	01:17	01:18
Axial multiphase T1 TP	00:11	00:12	00:13	00:12
Axial DWI	01:28	01:28	03:42	02:00
Set-up time	10:00	10:00	10:00	10:00
Total AT Dyn-AMRI	16:09	16:11	17:50	16:06
Mean (range) AT Dyn-AMRI	16:24 (15:46–17:30)			

*T2 HASTE can be performed after contrast injection in Dyn-AMRI

AP1 1st arterial phase, *AP2* 2nd arterial phase, *AT* acquisition time, *DWI* diffusion-weighted imaging, *Dyn-AMRI* abbreviated MRI using dynamic contrast-enhanced sequences, *HBP* hepatobiliary phase, *HBP-AMRI* abbreviated MRI using HBP, *NC-AMRI* non-contrast abbreviated MRI, *PVP* portal venous phase, *TP* transitional phase, *wi* weighted imaging

considered HCC-negative. LI-RADS 5 features include a 10–19-mm nodule with non-rim arterial phase hyperenhancement and non-peripheral washout appearance, regardless of capsule appearance, or a ≥20-mm nodule with non-rim arterial phase enhancement with either enhancing capsule appearance or non-peripheral washout appearance or both. Because of the known limitation of the transitional phase for assessing washout with gadoxetate, readers were asked to diagnose washout only on the portal venous phase. As readers did not have access to previous imaging, threshold growth was not considered. Additionally, the study coordinator collected the clinical, biological, and any follow-up radiological data.

Reference standard

Each patient was classified as positive/negative for HCC by two different radiologists (N.V.V. and B.T., with 2 and 13 years of expertise in abdominal radiology, respectively) in consensus. Classification was based on the review of all available patient data including imaging exams, pathology, any subsequent treatment, and decision from the multidisciplinary tumour board. For all patients with negative screening exams, at least 6-month MRI follow-up was required to confirm the negative result. All follow-up data were reviewed and recorded through 31 December 2018. HCC diagnosis was based either on pathologic

confirmation or imaging characteristics for HCC, according to the current guidelines [23]. On imaging, patients with LI-RADS 5 lesions were considered HCC-positive. Patients with observations who scored LI-RADS 3, 4, and M were considered HCC-positive only when pathologic confirmation was available or if they developed LI-RADS 5 characteristics within 6 months. Patients were considered HCC-negative when no lesion was found on the index MRI and on follow-up MRI, or when all observations were scored as LI-RADS 1/2. Additionally, patients with LI-RADS 3, 4, and M observations on reference standard that were stable were classified as HCC-negative. Patients with missing reference standard (due to absence of follow-up ($n = 2$) or treatment without definite diagnosis ($n = 1$)) were excluded (Fig. 1). True positive was defined when the patient was HCC-positive on AMRI and on the reference standard. True negative was defined as HCC-negative on AMRI with no HCC according to the reference standard. False positive was defined as HCC-positive on AMRI and HCC-negative according to the reference standard. False negative was defined as HCC-negative on AMRI and HCC-positive according to the reference standard. False negative lesions included missed and mischaracterised lesions.

Statistical analysis

The diagnostic performance for HCC detection was calculated for each AMRI set. The comparisons in terms of sensitivity and specificity achieved by each reader relative to the reference standard diagnosis were based on the McNemar test. For all other comparisons, logistic regression for correlated data was used to compare the methods in terms of the predictive values achieved by each reader and in terms of all components of diagnostic accuracy pooled over the two readers. Generalised estimating equations based on binary logistic regression were used to model the diagnostic accuracy achieved using each set as a function of reader and set.

An anonymised subject ID was incorporated into the generalised estimating equations analysis as a random classification factor to allow results to be modelled as positively correlated when derived for the same patient and as independent when derived for different patients. Kappa coefficient (K) was used to assess agreement between readers. The level of agreement was interpreted as poor ($K < 0$), slight ($0 \le K \le 0.2$), fair ($0.2 < K \le 0.4$), moderate ($0.4 < K \le 0.6$), substantial ($0.6 < K \le 0.8$), or almost perfect ($K > 0.8$). p value < 0.05 was considered statistically significant. All statistical tests were conducted at the two-sided 5% significance level using SAS 9.4 software (SAS Institute).

Cost-effectiveness analysis

We created a microsimulation model of HCC natural history and surveillance among cirrhotic patients in the USA. In our state transition framework, 50,000 50-year-old cirrhotic patients progress through the health states representing the development and growth of HCC (based on an annual HCC risk of 5.5% as reported in our series), screening for these tumours (using semi-annual US until age 70), subsequent treatment, and long-term survival, considering both HCC-related and non-HCC mortality (supplemental materials). Transition parameters were derived from published data (supplemental materials) and each health state was associated with costs. The simulation was run on a lifetime horizon with costs from a payor's perspective and was calibrated to population-based data on mortality for persons with cirrhosis [24]. Identical cohorts were then simulated, undergoing HCC screening with each AMRI set (semi-annually until age 70) which provided data to compare life expectancy and costs. Test characteristics for each AMRI set were estimated using point estimates from the study. For US, we used published estimates from a prospective American study, which reported 44% detection sensitivity [18]. Costs of imaging tests were based on 2017 USA Medicare reimbursement fee, which was $142 for US. Cost of AMRI was obtained by dividing the technical and professional components by two (given the shorter table time and lower number of images to be interpreted) while keeping the contrast price unchanged as follows: complete diagnostic gadoxetate-enhanced MRI, $704 (including $115 for 10 mL of gadoxetate); NC-AMRI, $295; HBP-AMRI and Dyn-AMRI, both $409 (including contrast). We then calculated the differences in costs of each AMRI set compared with US. We also estimated differences in life years lived, i.e. incremental effectiveness. We repeated these simulations using different annual HCC prevalence (2% and 3%).

Results

Reference standard

The final study population included 237 patients (M/F 139/98, mean age 58 years). Patient demographics and clinical characteristics including the subgroup of patients with HCC are shown in Table 2. A total of 134 patients (56.5%) were listed for liver transplantation, including 15 patients (6.3%) with Child-Pugh class C. Of 237 patients, 59 presented with observations identified on the reference standard, including 13 patients with HCC (13/237, prevalence, 5.5%; mean age 67 ± 9 years; M/F, 11/2). Two patients presented with multiple HCC lesions: one had two tumours and the other patient had an index HCC with multiple satellite nodules. The 11 other patients presented with a single HCC lesion. The mean tumour size (considering the larger lesion in each patient) was 33.7 ± 30 mm (range 10–120 mm). The largest tumour (120 mm) was a biopsy-proven HCC. HCC and other observations found on MRI are detailed in Table 3. Eleven (84.6%) patients

Table 2 Demographic and clinical characteristics of the study cohort and subgroup of patients with HCC

Variable		Study cohort ($n = 237$)	Patients with HCC ($n = 13$)	p
Sex (M/F)		139/98	11/2	0.06
Age (mean ± SD, range) (years)		58 ± 11.9, 20–88	67 ± 8.5, 54–87	0.007
Aetiology of liver disease				
	Chronic HCV	61 (25.7%)	8 (61.5%)	0.005
	Chronic HBV	30 (12.7%)	0	
	NASH	53 (22.4%)	3 (23.1%)	
	Alcohol	39 (16.5%)	2 (15.4%)	
	Other*	54 (22.8%)	0	
Liver cirrhosis		207 (87.3%)	13 (100%)	0.17
Child-Pugh score				
	A	167 (70.5%)	7 (53.8%)	0.12
	B	41 (17.5%)	4 (30.8%)	
	C	15 (6.3)	2 (15.4%)	
	Unknown	14 (5.9%)	0	
Listed for liver transplantation		134 (56.5%)	6 (46.2%)	0.47

*Autoimmune hepatitis, primary biliary cirrhosis, primary sclerosing cholangitis, hemochromatosis, alpha-1 antitrypsin deficiency, cryptogenic

HCV hepatitis C virus, *HBV* hepatitis B virus, *NASH* non-alcoholic steatohepatitis

had early HCC according to the Milan criteria [25]. Lesions were located (largest lesion) in segment II ($n = 1$), segment III ($n = 1$), segment IV ($n = 2$), segment V ($n = 1$), segment VI ($n = 2$), segment VII ($n = 2$), and segment VIII ($n = 4$).

Compared with the whole cohort, patients in the HCC subgroup were older, more likely to be male, and more frequently had chronic HCV as aetiology of liver disease (Table 2). The mean weight-based gadoxetate dose was 0.031 ± 0.09 mmol/kg (range 0.014–0.058 mmol/kg).

HCC detection (Table 4)

The inter-reader agreement for HCC detection was substantial for NC-AMRI ($K = 0.76$) and HBP-AMRI ($K = 0.75$), and almost perfect for Dyn-AMRI ($K = 0.86$). Table 4 shows the diagnostic performance of each reader for each set including pairwise comparison between each set for each reader and the pooled reader data (Fig. 2). Specificity and positive predictive value were significantly higher with Dyn-AMRI compared

Table 3 Description of liver observations (59 patients) in the study population

Observations	LI-RADS score	n
HCC		13
	LI-RADS 5	11
	LI-RADS 4, confirmed HCC at 6 months	1
	LI-RADS M, biopsy-proven HCC	1
Cholangiocarcinoma	LI-RADS M	1
Benign		18
Haemangioma	LI-RADS 1	8
Hepatocellular adenoma	LI-RADS 5	1
Presumed dysplastic nodules	LI-RADS 2	5
Focal fat	LI-RADS 1	1
Perfusion alterations	LI-RADS 1/2	3
Indeterminate		**27**
	LI-RADS 3, stable at 6 months	25
	LI-RADS 4, stable at 1 year	1
	LI-RADS M, stable at 6 months, no pathological confirmation	1

LI-RADS Liver Imaging Reporting and Data System

with the two other sets ($p < 0.01$). No difference was found for sensitivity and negative predictive value (p range 0.06–0.64); however, the sample size precluded any meaningful comparison of sensitivity.

False positives

On NC-AMRI, there were 10 false positives for both readers. These were due to focal fat ($n = 1$), presumed dysplastic nodule ($n = 1$), LI-RADS 3 observations that remained stable at 6-month follow-up ($n = 4$), hepatocellular adenoma ($n = 1$), hepatic pseudo-lesion ($n = 1$), cholangiocarcinoma ($n = 1$), and an indeterminate lesion (LI-RADS M without histologic confirmation, $n = 1$). On HBP-AMRI, there were 12 false positives for reader 1 and 11 false positives for reader 2. These were due to the same observations as NC-AMRI except for the focal fat observation and additional presumed dysplastic nodule that were considered positive at HBP-AMRI. The one false positive (reader 2) for Dyn-AMRI was a hepatocellular adenoma. No false positive was recorded with Dyn-AMRI with reader 1.

False negatives

Missed HCCs were small, with a mean size of 15 ± 3.7 mm (range, 10–19 mm), except for a 120-mm lesion that was mischaracterised with Dyn-AMRI.

All false negative lesions included missed lesions with NC-AMRI and HBP-AMRI.

On NC-AMRI, the same 5 HCCs were missed by reader 1 and reader 2 (mean size, 15 mm; range, 10–19 mm). All HCCs missed on HBP-AMRI were missed on NC-AMRI. Three HCCs were missed by reader 1 (mean size, 14 mm; range, 10–19 mm) and 2 HCCs were missed by reader 2 (10 and 13 mm) on HBP-AMRI (Fig. 3). On Dyn-AMRI, reader 1 missed one lesion (13 mm) and mischaracterised 2 HCC lesions (scored LI-RADS 4 (10 mm) and LI-RADS M (120 mm)). Reader 2 mischaracterised 1 HCC as LI-RADS M (120 mm).

Cost-effectiveness analysis (Table 5)

All AMRI sets were effective compared with semi-annual US, under any HCC prevalence assumptions. Dyn-AMRI and HBP-AMRI were the most effective strategies in all three scenarios. Incremental costs compared to US were $11,823, $11,606, and $11,494 for NC-AMRI, HBP-AMRI, and Dyn-AMRI, respectively. They were associated with population-level life-year gains of 12/9, 7/6, and 5/4 months for Dyn-AMRI/HBP-AMRI with 5.5%, 3%, and 2% HCC annual prevalence, respectively, compared with US.

Discussion

In this study, we compared the diagnostic performance of 3 AMRI sets extracted from a complete gadoxetate-enhanced MRI exam, including NC-AMRI, HBP-AMRI, and Dyn-AMRI. We found no difference between sets with regard to sensitivity or negative predictive value, while specificity and

Table 4 Per-patient diagnostic performance for each AMRI set for HCC detection with 95% confidence intervals and pairwise comparisons

Reader	Method	Sensitivity (ratio, 95% CI)	Specificity (ratio, 95% CI)	PPV (ratio, 95% CI)	NPV (ratio, 95% CI)
1*	NC-AMRI	61.5% (8/13, 31.6–86.1%)	95.5% (214/224, 91.9–97.8%)	44.4% (21.5–69.8%)	97.7% (94.8–99.3%)
	HBP-AMRI	76.9% (10/13, 46.2–95%)	94.6% (212/224, 90.8–97.2%)	45.5% (24.4–67.8%)	98.6% (96–99.7%)
	Dyn-AMRI	76.9% (10/13, 46.2–95%)	100% (224/224, 98.4–100%)	100% (69.2–100%)	98.7% (96.2–99.7%)
	p (NC-AMRI vs. HBP-AMRI)	0.157	0.414	0.888	0.478
	p (NC-AMRI vs. Dyn-AMRI)	0.317	*0.002*	*< 0.001*	0.445
	p (HBP-AMRI vs. Dyn-AMRI)	1	*< 0.001*	*< 0.001*	0.921
2**	NC-AMRI	61.5% (8/13, 31.6–86.1%)	95.5 (214/224, 91.9–97.8%)	44.4% (21.5–69.2%)	97.7% (94.8–99.3%)
	HBP-AMRI	84.6% (11/13, 54.6–98.1%)	95.1 (213/224, 91.4–97.5%)	50% (28.2–71.8%)	99.1% (96.7–99.9%)
	Dyn-AMRI	92.3% (12/13, 64–99.8%)	99.6 (223/224, 97.5–100%)	92.3% (64–99.8%)	99.6% (97.5–100%)
	p (NC-AMRI vs. HBP-AMRI)	0.083	0.739	0.333	0.501
	p (NC-AMRI vs. Dyn-AMRI)	0.102	*0.003*	*0.002*	0.423
	p (HBP-AMRI vs. Dyn-AMRI)	0.564	*0.002*	*0.001*	0.911
Pooled data	NC-AMRI	61.5% (34.4–83%)	95.5% (92.4–97.4%)	44.4% (24.8–66%)	97.7% (94.6–99%)
	HBP-AMRI	80.8% (53.6–93.9%)	94.9% (91.6–96.9%)	47.7% (29.3–66.8%)	98.8% (96.3–99.6%)
	Dyn-AMRI	84.6% (60.8–95.1%)	99.8% (98.4–100%)	95.7% (74–99.4%)	99.1% (97.1–99.7%)
	p (NC-AMRI vs. HBP-AMRI)	0.06	0.548	0.644	0.186
	p (NC-AMRI vs. Dyn-AMRI)	0.126	*0.002*	*0.001*	0.117
	p (HBP-AMRI vs. Dyn-AMRI)	0.7	*0.001*	*0.001*	0.637

*3 years of experience, **10 years of experience

CI confidence intervals, *PPV* positive predictive value, *NPV* negative predictive value, *NC-AMRI* non-contrast abbreviated MRI, *HBP-AMRI* abbreviated MRI using hepatobiliary phase, *Dyn-AMRI* abbreviated MRI using dynamic contrast-enhanced sequences

All significant values are in italic

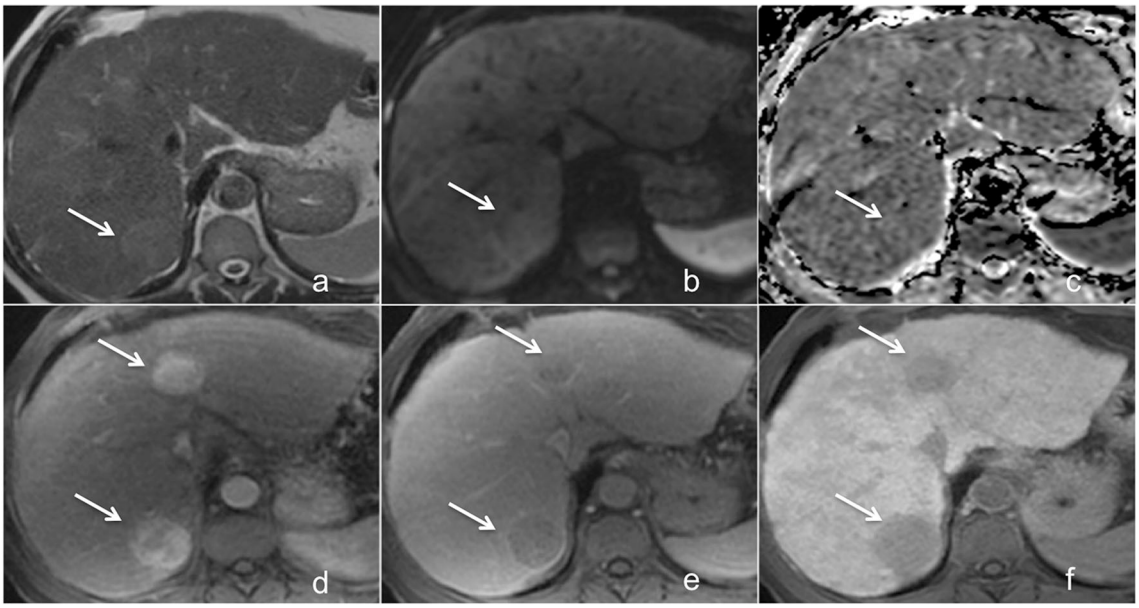

Fig. 2 A 60-year-old male patient with HCV cirrhosis and bifocal HCC in segments 4A and 7. **a** Axial T2wi shows a mildly hyperintense lesion in segment 7 (arrow) with corresponding mild hyperintensity on diffusion-weighted images (b800) with isointensity on apparent diffusion coefficient map (**b** and **c**, arrows). Axial T1wi obtained at the arterial (**d**), portal venous (**e**), and hepatobiliary phases (**f**) demonstrates 4.0-cm lesion in segment 7 with arterial phase hyperenhancement (**d**), washout/capsule (**e**), and hypointensity on hepatobiliary phase (**f**, arrows). Note the presence of a second lesion in segment 4A, seen only on contrast-enhanced images (**d**–**f**, arrows). Readers scored NC-AMRI, HBP-AMRI, and Dyn-AMRI (LI-RADS 5) as positive. Wi, weighted imaging; AMRI, abbreviated MRI; NC, non-contrast; HBP, hepatobiliary phase; Dyn, dynamic

positive predictive value were higher with Dyn-AMRI compared with NC-AMRI and HBP-AMRI. Based on American data, we also performed a preliminary cost-effectiveness analysis comparing the 3 AMRI sets to US, which revealed that all AMRI sets were effective compared with US.

Although specific, NC-AMRI had low sensitivity (61.5%). This contradicts promising results of NC-AMRI incorporating DWI for HCC detection [9, 12]. Our results suggest that gadolinium contrast is needed to achieve acceptable sensitivity for AMRI-based HCC screening [10, 16]. However, from our clinical practice, including T2wi with/without DWI may be needed for benign lesion characterisation. Larger series on HCC screening population including serial surveillance exams are needed to investigate the superiority of contrast-enhanced AMRI compared with NC-AMRI. Compared with HBP-AMRI, Dyn-AMRI had slightly higher specificity (99.8% vs. 94.9%), while the absence of difference in sensitivity and negative predictive value may be related to sample size.

Dyn-AMRI was extracted from a complete gadoxetate-enhanced MRI. We envision that if Dyn-AMRI was performed for clinical care, one could utilise an extracellular contrast agent (ECCA), which would be expected to provide equal or higher performance than gadoxetate for the following reasons: (1) higher dose of gadolinium injected (0.1 mmol/kg for ECCA vs. 0.03 mmol/kg of gadoxetate on average in our series); (2) lower rates of artefacts at the arterial phase (2% with ECCA vs. 17% with gadoxetate as reported previously) [26]; (3) more flexible characterisation of "washout" in either the portal venous or equilibrium phase with ECCA vs. constrained to the portal venous phase with gadoxetate [27]. In addition, the advantages of HBP may not be fully realised in patients with chronic liver disease due to the possibility of decreased uptake of gadoxetate in patients with advanced hepatic dysfunction. Furthermore, Dyn-AMRI using ECCA has several theoretical advantages over HBP-AMRI: (1) it allows HCC detection and characterisation during the same exam, which is not possible with NC-AMRI and HBP-AMRI, (2) cost of ECCA is generally lower than gadoxetate. On the other hand, when compared with dynamic imaging, HBP was shown to improve lesion conspicuity and lesion-to-liver contrast ratio, particularly for detection of early HCC [28, 29]. Only 2 studies have reported the use of Dyn-AMRI protocols for HCC detection using ECCA [16, 17], and both found high concordance in LI-RADS 5 diagnosis between Dyn-AMRI and the complete MRI exam.

Our results with NC-AMRI are in the lower range for sensitivity compared with previous published data that showed sensitivity of 79.1–91.7% [9, 10, 12]. These differences may relate to the study population. The present study was based on a screening population while two out of three of these previous studies [9, 10] included a population with higher HCC prevalence (35.6% and 85.9% vs. 5.5% in the present study). HBP-AMRI performance in the present study is similar to previous studies which reported sensitivity of 79.6–85.7% and specificity of 91.2–96.1% [10, 13, 14].

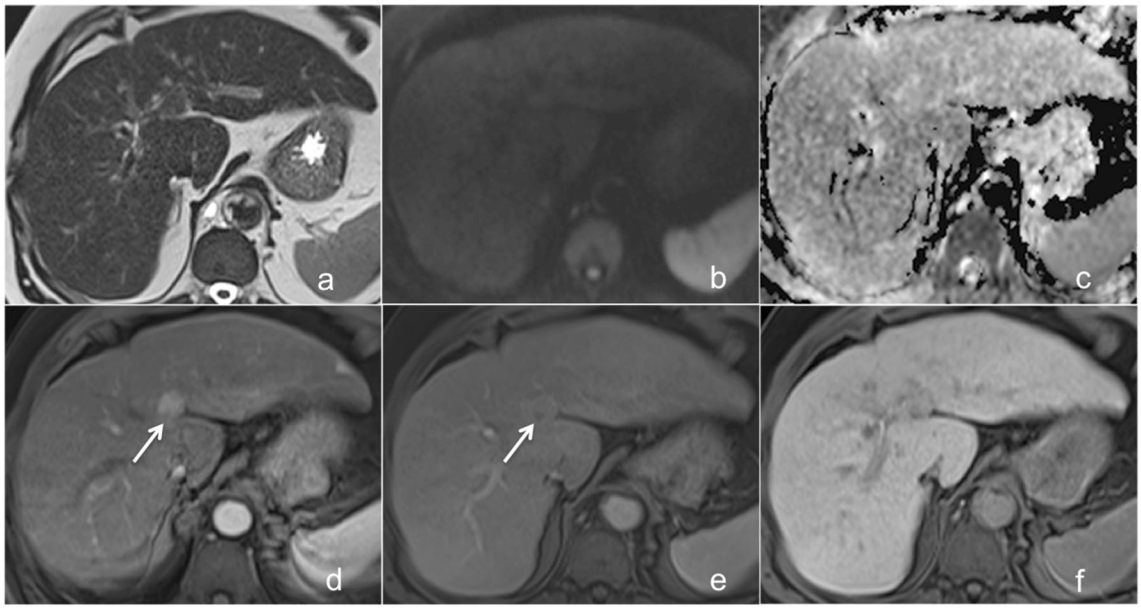

Fig. 3 A 67-year-old male patient with chronic HBV cirrhosis and HCC. **a** Axial T2wi and (**b**) axial diffusion-weighted images (b800) and corresponding apparent diffusion coefficient map (**c**) show no discernible lesion. Axial T1wi obtained at the arterial (**d**) and portal venous (**e**) phases demonstrates 18-mm lesion with arterial phase hyperenhancement (**d**) in segment 4 with washout and enhancing capsule (**e**, arrows). The lesion is not clearly identified on T1w obtained at the hepatobiliary phase (**f**). Readers scored NC-AMRI and HBP-AMRI as negative and positive (LI-RADS 5) on Dyn-AMRI. Wi, weighted imaging; AMRI, abbreviated MRI; NC, non-contrast; HBP, hepatobiliary phase; Dyn, dynamic

AMRI allows a substantial reduction in acquisition time compared with a complete MRI, with high patient and radiologist acceptance (although not measured in our study). According to our protocols, NC-AMRI and HBP-AMRI protocols can be performed in less than 14 min (including set-up), while Dyn-AMRI is a bit longer (around 16 min). As Marks et al showed no added value of DWI for HCC detection using HBP-AMRI [13], we suggest that Dyn-AMRI could be performed without DWI with subsequent reduction in acquisition time. In addition, compared with NC-AMRI and HBP-AMRI that require no contrast injection or injection outside the exam room, Dyn-AMRI requires contrast injection using an automated contrast injector with slightly longer table time. We estimated the set-up time to be approximately 10 min, which is realistic based on our clinical experience. In addition to the reduction in acquisition time, AMRI allows reduction in interpretation time due to the reduction of sequence acquisition, which has also to be weighted for the cost-effectiveness analysis.

Table 5 Cost effectiveness analysis for each AMRI set in comparison with US used as the reference.

	Incremental costs (in United States $ with ranges*)		
Simulation output	2% HCC prevalence	3% HCC prevalence	5.5% HCC prevalence
Ultrasound**	Reference		
NC-AMRI	$15,429.42 (11,875.37-dominated***)	$14,130.37 (11,548.32-dominated***)	$11,823.17 (11,771.11-dominated***)
HBP-AMRI	$12,900.47 (11,956.83-18,300.24)	$11,974.52 (11,878.95-15,128.91)	$11,606.92 (11,137.31-13,067.08)
Dyn-AMRI	$11,810.74 (11,668.77-12,379.53)	$12,146.2 (11,997.56-11,319.40)	$11,494.21 (11,280.73-12,274.14)
	Overall survival benefit associated compared with US in months (ranges*)		
NC-AMRI	1.2 (dominated*** - 4.3)	1.8 (dominated*** - 5.9)	3.4 (dominated*** - 9.4)
HBP-AMRI	3.9 (1 - 5.6)	5.8 (1.5-7.9)	9.3 (2.4-12.8)
Dyn-AMRI	5.2 (3.5-5.8)	6.8 (5.3-8.3)	11.6 (7.5-13.4)

*Ranges are based on sensitivity 95% confidence intervals from study test characteristic findings. **US diagnostic performance is based on published estimates from a prospective American study, which reported 44% detection sensitivity [18]. ***Dominated means no survival benefit

HCC hepatocellular carcinoma, *NC-AMRI* non-contrast abbreviated MRI, *HBP-AMRI* abbreviated MRI using hepatobiliary phase, *Dyn-AMRI* abbreviated MRI using dynamic contrast-enhanced sequences

Goossens et al highlighted the lack of cost-effectiveness of the current HCC screening recommendation with US [30]. By building models including HCC screening with AMRI only for patients with intermediate to high HCC risk, the same group showed the potential cost-effectiveness of HBP-AMRI for HCC screening [30]. Lima et al compared HCC screening performed with different scenarios including US, CT, complete MRI, and AMRI and concluded that HCC screening performed with AMRI was cost-effective in a conservative scenario (52% surveillance compliance) [31]. We found similar results in our analysis; AMRI-based models were cost-effective compared with US with incremental costs well within currently accepted ranges (< $50,000) [32], although we did not model compliance. Due to their higher diagnostic performance compared with NC-AMRI, HBP-AMRI and Dyn-AMRI were the most cost-effective models, allowing population-level life-year gains of 7–12 months compared with US.

Our study has several limitations. First, due to its retrospective design, AMRI sets were reconstructed from a complete gadoxetate-enhanced MRI. Consequently, Dyn-AMRI did not mirror Dyn-AMRI performed with an ECCA. Second, a high percentage of our patient population was listed on liver transplant list (56.6%), which may not necessarily apply to non-transplant centres. This may explain the relatively high prevalence of HCC (5.5%) in our study population, potentially leading to overestimation of AMRI performance compared with a lower prevalence population. Third, we used the LI-RADS algorithm for both Dyn-AMRI and reference standard that could bias results in favour of Dyn-AMRI. However, while Dyn-AMRI assessment was based on reading of one imaging set, reference standard was based on all available imaging data and patient information. Fourth, our cost-effectiveness analysis is based on literature values for US sensitivity, as we were not able to perform a comparison with US. We based our choice on a prospective study performed on a screening cohort in the USA in order to match our study population as closely as possible, but underlying differences between the study populations may have confounded the cost-effectiveness analysis [18]. Prospective head-to-head comparisons of the diagnostic performance and cost-effectiveness of AMRI and US as well as assessment of the added value of blood biomarkers are needed. Initial prospective data, comparing NC-AMRI to US in Korea, is in favour of NC-AMRI [12]. Additionally, we acknowledge that our cost-effectiveness assessment is based on USA cost estimates and is not generalizable to other countries due to differences in healthcare models and costs. However, this was provided as a model to be tested in other systems.

In conclusion, contrast-enhanced AMRI demonstrated better diagnostic performance for HCC screening compared with NC-AMRI. HBP-AMRI and Dyn-AMRI had similar diagnostic performance and cost-effectiveness with slightly higher specificity for Dyn-AMRI. Future prospective studies, including direct comparison with US, are needed to confirm these results.

Funding information Naik Vietti Violi: Swiss National Science Foundation, fellowship P2LAP3_178053. The authors state no other funding for this work.

Compliance with ethical standards

Guarantor The scientific guarantor of this publication is Bachir Taouli.

Conflict of interest The authors of this manuscript declare relationships with the following companies:

Claude B. Sirlin:

Industry research support: Bayer Healthcare, GE, Gilead, Philips, Siemens.

Consulting: Epigenomics

Institutional Consulting Representative: IBM-Watson

Mustafa R. Bashir:

Research grants: Siemens, NGM Biopharmaceuticals, Madrigal Pharmaceuticals, Metacrine Inc., ProSciento, Pinnacle Clinical Research, CymaBay Therapeutics

Consulting: MedPace

Kathryn J. Fowler:

Research grants: Bayer Healthcare, GE, Pfizer

Consulting: Epigenomics, 12 sigma, Medscape, Bayer Healthcare

Bachir Taouli:

Research grants: Bayer Healthcare, Takeda

Consultant: Bayer Healthcare, Alexion

The other authors of this manuscript declare no relationships with any companies, whose products or services may be related to the subject matter of the article.

Statistics and biometry One of the authors has significant statistical expertise. It is JS Babb.

Informed consent Written informed consent was waived by the Institutional Review Board.

Ethical approval Institutional Review Board approval was obtained.

Methodology

- retrospective
- case-control study
- performed at one institution

References

1. Ryerson AB, Eheman CR, Altekruse SF et al (2016) Annual Report to the Nation on the Status of Cancer, 1975-2012, featuring the increasing incidence of liver cancer. Cancer 122:1312–1337
2. Marrero JA, Kulik LM, Sirlin CB et al (2018) Diagnosis, staging, and management of hepatocellular carcinoma: 2018 practice guidance by the American Association for the Study of Liver Diseases. Hepatology 68:723–750
3. European Association for the Study of the Liver (2018) EASL clinical practice guidelines: management of hepatocellular carcinoma. J Hepatol 69:182–236

4. Kim SY, An J, Lim YS et al (2017) MRI with liver-specific contrast for surveillance of patients with cirrhosis at high risk of hepatocellular carcinoma. JAMA Oncol 3:456–463
5. Tzartzeva K, Obi J, Rich NE et al (2018) Surveillance imaging and alpha fetoprotein for early detection of hepatocellular carcinoma in patients with cirrhosis: a meta-analysis. Gastroenterology 154: 1706–1718 e1701
6. Arguedas MR, Chen VK, Eloubeidi MA, Fallon MB (2003) Screening for hepatocellular carcinoma in patients with hepatitis C cirrhosis: a cost-utility analysis. Am J Gastroenterol 98:679–690
7. Colli A, Fraquelli M, Casazza G et al (2006) Accuracy of ultrasonography, spiral CT, magnetic resonance, and alpha-fetoprotein in diagnosing hepatocellular carcinoma: a systematic review. Am J Gastroenterol 101:513–523
8. Canellas R, Rosenkrantz AB, Taouli B et al (2019) Abbreviated MRI protocols for the abdomen. Radiographics 39:744–758
9. Kim YK, Kim YK, Park HJ, Park MJ, Lee WJ, Choi D (2014) Noncontrast MRI with diffusion-weighted imaging as the sole imaging modality for detecting liver malignancy in patients with high risk for hepatocellular carcinoma. Magn Reson Imaging 32:610–618
10. Besa C, Lewis S, Pandharipande PV et al (2017) Hepatocellular carcinoma detection: diagnostic performance of a simulated abbreviated MRI protocol combining diffusion-weighted and T1-weighted imaging at the delayed phase post gadoxetic acid. Abdom Radiol (NY) 42:179–190
11. Chan MV, McDonald SJ, Ong YY et al (2019) HCC screening: assessment of an abbreviated non-contrast MRI protocol. Eur Radiol Exp 3:49
12. Park HJ, Jang HY, Kim SY et al (2020) Non-enhanced magnetic resonance imaging as a surveillance tool for hepatocellular carcinoma: comparison with ultrasound. J Hepatol 72:718–724
13. Marks RM, Ryan A, Heba ER et al (2015) Diagnostic per-patient accuracy of an abbreviated hepatobiliary phase gadoxetic acid-enhanced MRI for hepatocellular carcinoma surveillance. AJR Am J Roentgenol 204:527–535
14. Tillman BG, Gorman JD, Hru JM et al (2018) Diagnostic per-lesion performance of a simulated gadoxetate disodium-enhanced abbreviated MRI protocol for hepatocellular carcinoma screening. Clin Radiol 73:485–493
15. Park SH, Kim B, Kim SY et al (2020) Abbreviated MRI with optional multiphasic CT as an alternative to full-sequence MRI: LI-RADS validation in a HCC-screening cohort. Eur Radiol 30: 2302–2311
16. Lee JY, Huo EJ, Weinstein S et al (2018) Evaluation of an abbreviated screening MRI protocol for patients at risk for hepatocellular carcinoma. Abdom Radiol (NY) 43:1627–1633
17. Khatri G, Pedrosa I, Ananthakrishnan L et al (2019) Abbreviated-protocol screening MRI vs. complete-protocol diagnostic MRI for detection of hepatocellular carcinoma in patients with cirrhosis: an equivalence study using LI-RADS v2018. J Magn Reson Imaging. https://doi.org/10.1002/jmri.26835
18. Singal AG, Conjeevaram HS, Volk ML et al (2012) Effectiveness of hepatocellular carcinoma surveillance in patients with cirrhosis. Cancer Epidemiol Biomarkers Prev 21:793–799
19. Park MS, Kim S, Patel J et al (2012) Hepatocellular carcinoma: detection with diffusion-weighted versus contrast-enhanced magnetic resonance imaging in pretransplant patients. Hepatology 56: 140–148
20. McNamara MM, Thomas JV, Alexander LF et al (2018) Diffusion-weighted MRI as a screening tool for hepatocellular carcinoma in cirrhotic livers: correlation with explant data-a pilot study. Abdom Radiol (NY). https://doi.org/10.1007/s00261-018-1535-y
21. Morgan TA, Maturen KE, Dahiya N et al (2018) US LI-RADS: ultrasound Liver Imaging Reporting and Data System for screening and surveillance of hepatocellular carcinoma. Abdom Radiol (NY) 43:41–55
22. Ito K, Honjo K, Fujita T, Awaya H, Matsumoto T, Matsunaga N (1996) Hepatic parenchymal hyperperfusion abnormalities detected with multisection dynamic MR imaging: appearance and interpretation. J Magn Reson Imaging 6:861–867
23. Wald C, Russo MW, Heimbach JK, Hussain HK, Pomfret EA, Bruix J (2013) New OPTN/UNOS policy for liver transplant allocation: standardization of liver imaging, diagnosis, classification, and reporting of hepatocellular carcinoma. Radiology 266:376–382
24. van der Meer AJ, Wedemeyer H, Feld JJ et al (2014) Life expectancy in patients with chronic HCV infection and cirrhosis compared with a general population. JAMA 312:1927–1928
25. Mazzaferro V, Regalia E, Doci R et al (1996) Liver transplantation for the treatment of small hepatocellular carcinomas in patients with cirrhosis. N Engl J Med 334:693–699
26. Davenport MS, Viglianti BL, Al-Hawary MM et al (2013) Comparison of acute transient dyspnea after intravenous administration of gadoxetate disodium and gadobenate dimeglumine: effect on arterial phase image quality. Radiology 266:452–461
27. Cruite I, Schroeder M, Merkle EM, Sirlin CB (2010) Gadoxetate disodium-enhanced MRI of the liver: part 2, protocol optimization and lesion appearance in the cirrhotic liver. AJR Am J Roentgenol 195:29–41
28. Bashir MR, Gupta RT, Davenport MS et al (2013) Hepatocellular carcinoma in a North American population: does hepatobiliary MR imaging with Gd-EOB-DTPA improve sensitivity and confidence for diagnosis? J Magn Reson Imaging 37:398–406
29. Besa C, Kakite S, Cooper N, Facciuto M, Taouli B (2015) Comparison of gadoxetic acid and gadopentetate dimeglumine-enhanced MRI for HCC detection: prospective crossover study at 3 T. Acta Radiol Open 4:2047981614561285
30. Goossens N, Singal AG, King LY et al (2017) Cost-effectiveness of risk score-stratified hepatocellular carcinoma screening in patients with cirrhosis. Clin Transl Gastroenterol 8:e101
31. Lima PH, Fan B, Berube J et al (2019) Cost-utility analysis of imaging for surveillance and diagnosis of hepatocellular carcinoma. AJR Am J Roentgenol. https://doi.org/10.2214/AJR.18.20341:1-9
32. Neumann PJ, Cohen JT, Weinstein MC (2014) Updating cost-effectiveness–the curious resilience of the $50,000-per-QALY threshold. N Engl J Med 371:796–797